http://www.kidney-international.org

Amiloride blocks lithium entry through the sodium channel thereby attenuating the resultant nephrogenic diabetes insipidus

Marleen L.A. Kortenoeven[1,4], Yuedan Li[1,4], Stephen Shaw[1], Hans-Peter Gaeggeler[3], Bernard C. Rossier[3], Jack F.M. Wetzels[2] and Peter M.T. Deen[1]

[1]Department of Physiology, Radboud University Nijmegen Medical Centre, Nijmegen, The Netherlands; [2]Department of Nephrology, Radboud University Nijmegen Medical Centre, Nijmegen, The Netherlands and [3]Département de Pharmacologie et de Toxicologie, Universite de Lausanne, Lausanne, Switzerland

Lithium therapy frequently induces nephrogenic diabetes insipidus; amiloride appears to prevent its occurrence in some clinical cases. Amiloride blocks the epithelial sodium channel (ENaC) located in the apical membrane of principal cells; hence one possibility is that ENaC is the main entry site for lithium and the beneficial effect of amiloride may be through inhibiting lithium entry. Using a mouse collecting duct cell line, we found that vasopressin caused an increase in Aquaporin 2 (AQP2) expression which was reduced by clinically relevant lithium concentrations similar to what is seen with *in vivo* models of this disease. Further amiloride or benzamil administration prevented this lithium-induced downregulation of AQP2. Amiloride reduced transcellular lithium transport, intracellular lithium concentration, and lithium-induced inactivation of glycogen synthase kinase 3β. Treatment of rats with lithium downregulated AQP2 expression, reduced the principal-to-intercalated cell ratio, and caused polyuria, while simultaneous administration of amiloride attenuated all these changes. These results show that ENaC is the major entry site for lithium in principal cells both *in vitro* and *in vivo*. Blocking lithium entry with amiloride attenuates lithium-induced diabetes insipidus, thus providing a rationale for its use in treating this disorder.

Kidney International (2009) **76,** 44–53; doi:10.1038/ki.2009.91; published online 15 April 2009

KEYWORDS: amiloride; aquaporin 2; ENaC; lithium; mCCD; nephrogenic diabetes insipidus

Correspondence: *Peter M.T. Deen, 286, Department of Physiology, Radboud University Nijmegen Medical Centre, PO Box 9101, Nijmegen 6500 HB, The Netherlands. E-mail: P.Deen@ncmls.ru.nl*

[4]These authors contributed equally to this work.

Received 27 August 2008; revised 21 January 2009; accepted 10 February 2009; published online 15 April 2009

Lithium is regularly used to treat psychiatric diseases, such as bipolar disorders, schizoaffective disorders, and depression. Lithium is prescribed to 0.1% of the population.[1] Approximately 20% of patients develop nephrogenic diabetes insipidus (NDI), a disorder characterized by polyuria and polydipsia because of renal insensitivity to the antidiuretic hormone, arginine vasopressin (AVP).[2] Thus, lithium-NDI is the most common form of NDI. Lithium-NDI patients are at risk for dehydration-induced lithium toxicity, and prolonged lithium treatment might lead to end-stage renal disease.[1] However, as the symptoms of the underlying psychiatric disorder have a high impact on the quality of life, cessation of lithium therapy is not an option for most patients.

The kidney is the main organ for regulating water homeostasis. In the state of hypernatremia or hypovolemia, AVP is released from the pituitary gland. Binding of AVP to the vasopressin type-2 receptor in the basolateral membrane of renal collecting duct principal cells results in the redistribution of aquaporin-2 (AQP2) water channels from intracellular vesicles to the apical membrane. Driven by an osmotic gradient, water will enter the principal cells through AQP2 and will exit through AQP3 or AQP4 in the basolateral membrane, resulting in the concentrated urine. Besides this short-term regulation, AVP also exerts a long-term regulation by increasing AQP2 expression.[3]

From studies in rats, it became clear that lithium-NDI develops in two stages. In the short term (10 days), lithium-NDI coincides with AQP2 downregulation and natriuresis, without gross changes in renal morphology.[4–6] Chronic lithium treatment (4 weeks), however, also leads to a severe decrease in the fraction of principal cells. This is 'compensated' by an increase in the fraction of intercalated cells, which are involved in acid/base balance regulation.[7,8]

Presently, it is unclear how lithium causes NDI and whether lithium-NDI can be attenuated. Some data, however, suggest that lithium may exert its effects by entering principal cells through the epithelial sodium channel (ENaC). First, NDI is due to an impaired water reabsorption in the connecting tubules and collecting ducts principal cells,[9] where ENaC

is expressed.[10] Second, ENaC has a higher permeability for lithium than for sodium.[11] Third, lithium inhibits amiloride-sensitive sodium reabsorption in the toad urinary bladder and rat collecting duct, tissues known to express ENaC,[12–14] and the ENaC-blocker triamterene increases lithium excretion.[15] Moreover, it was shown in a limited number of lithium-NDI patients that blocking ENaC with amiloride significantly reduces urine volume and increases urine osmolality.[16–18] The decreased urine volume is classically explained by an amiloride-induced hypovolemia, followed by an increased proximal sodium and water retention. The increased urine osmolality was suggested to be caused by an amiloride-induced reduction of sodium reabsorption.[16,17]

On the basis of the above, we hypothesized that lithium enters the principal cells through ENaC and that blocking ENaC by amiloride would reduce cellular entry of lithium, AQP2 downregulation, and alterations in the cellular composition of the collecting duct and the lithium-NDI phenotype.

RESULTS

mCCD$_{c11}$ cells as a model for lithium-NDI

To study the role of ENaC in lithium-NDI *in vitro*, a cell line needs to show (1) expression of all three ENaC subunits, (2) amiloride-inhibitable transcellular sodium transport, (3) deamino-8-D-arginine vasopressin (dDAVP)-induced expression of AQP2, and (4) lithium-induced downregulation of AQP2.

mpkCCD$_{cl4}$ cells show a lithium-induced AQP2 downregulation[19] and an amiloride-inhibitable transcellular voltage difference. However, immunocytochemistry did not reveal ENaC expression in these cells (data not shown), in contrast to the novel mouse cortical collecting duct mCCD$_{c11}$ cell line.[20] Therefore, we tested mCCD$_{cl1}$ cells as a model. To test whether dDAVP induces AQP2 expression in these cells, confluent cells were treated for 1–4 days with 1 nM dDAVP. Immunoblotting revealed the typical non-glycosylated 29 and complex-glycosylated 40–45 kDa AQP2 bands, besides a nonspecific band of 35 kDa (Figure 1a). Similar to mpkCCD$_{c14}$ cells,[19] maximal expression of AQP2 was observed after 72–96 h. To have steady AQP2 expression, cells were therefore treated with dDAVP for 96 h in the following experiments.

In patients on lithium therapy, the concentration of lithium is ~1 mM in serum and ranges between 1 and 10 mM in urine.[1] To test whether these concentrations affect AQP2 expression, cells were incubated with 1 mM lithium at the basolateral side and with either 1 or 10 mM lithium at the apical side for 24 or 48 h. Immunoblotting revealed that lithium reduced the AQP2 expression in a time- and dose-dependent manner, with an almost complete absence of AQP2 after a 48-h incubation in 10 mM lithium (Figure 1b). This concentration of lithium did not affect cell viability as indicated by similar coomassie-stained protein levels (Figure 1b) and a consistent transcellular resistance of $>1000\,\Omega/cm^2$ (data not shown). Together, these data reveal that mCCD$_{cl1}$ cells are a suitable model to investigate the role of ENaC in lithium-NDI.

The role of ENaC in AQP2 downregulation and transcellular lithium transport

ENaC is located in the apical membrane of collecting duct and mCCD$_{c11}$ cells,[20] and its activity is blocked by amiloride. To test whether ENaC mediates AQP2 downregulation by lithium, mCCD$_{c11}$ cells were treated for 48 h with lithium at only the basolateral (1 mM) or the apical (10 mM) side with or without amiloride. Application of lithium at the apical side reduced AQP2 expression to ~30% of control values, which

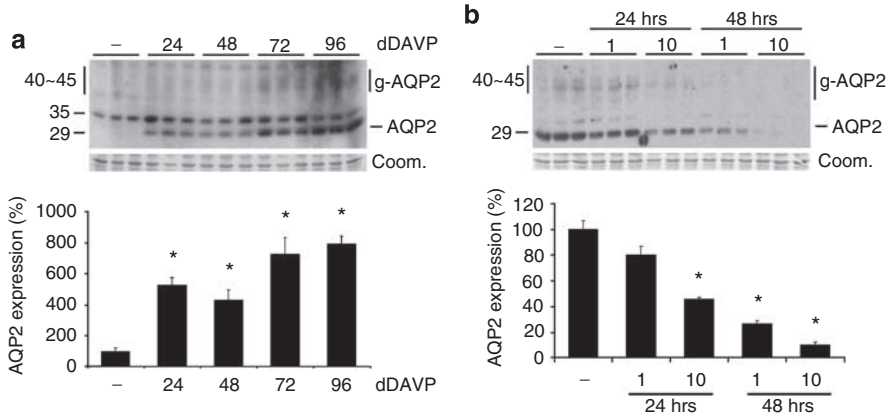

Figure 1 | mCCD$_{c11}$ cells: a proper cell model to study lithium-NDI. (**a**) mCCD$_{c11}$ cells were grown to confluence, treated for the indicated times (in hours) with 1 nM dDAVP, and subjected to AQP2 immunoblotting or, after blotting, stained with coomassie blue. Non-glycosylated (29 kDa) and complex-glycosylated (40–45 kDa) forms of AQP2, and an a-specific band of 35 kDa, are detected. (**b**) mCCD$_{c11}$ cells grown as previously described were treated for 96 h with 1 nM dDAVP, and for the last 24 or 48 h, in the absence (–) or presence of 1 mM lithium at the basolateral side and 1 or with 10 mM lithium at the apical side. Cells were lysed and immunoblotted for AQP2. Blots were also stained with coomassie blue. Molecular masses (in kDa) are indicated on the left. The signals for non-glycosylated and complex-glycosylated AQP2 were densitometrically quantified and normalized for coomassie blue staining. Mean values of normalized AQP2 expression per condition are given as the percentage of control (± s.e.m.) and were determined from three independent filters per condition. Significant differences ($P<0.05$) from control (–) are indicated by an asterisk.

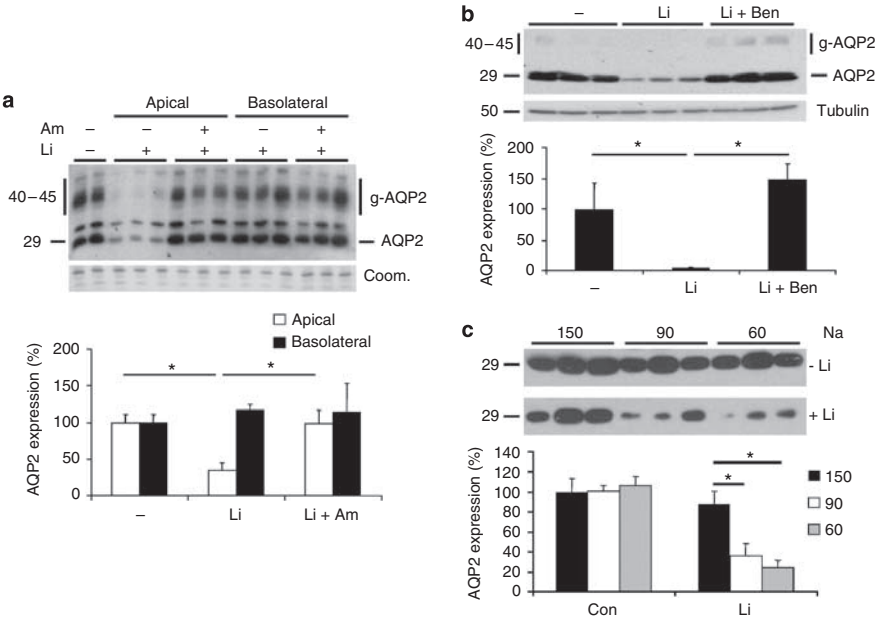

Figure 2 | ENaC blockers reduce lithium-induced AQP2 downregulation in $mCCD_{c11}$ cells. (**a**) Confluent $mCCD_{c11}$ monolayers were treated for 96 h with 1 nM dDAVP and incubated for the last 48 h in the absence (−) or presence (+) of lithium and/or with 10 μM amiloride as indicated. At the basolateral and apical side, 1 and 10 mM lithium were used, respectively. (**b**) Confluent $mCCD_{c11}$ monolayers were treated described earlier with 10 mM lithium with/without 10 μM benzamil (Li + Ben) at the apical side for the last 24 h. (**c**) $mCCD_{c11}$cells were grown as previously described and treated for the last 12 h in medium containing a lower sodium chloride concentration at the apical side only, with or without lithium (indicated). (**a**–**c**) Cells were lysed and immunoblotted for AQP2. Molecular masses (in kDa) are indicated on the left. Semiquantification of the AQP2 signals, normalization, and statistical analysis were carried out as described in the Figure 1 caption. Mean values were determined from three independent filters per condition. Significant differences ($P<0.05$) are indicated by an asterisk.

was prevented by amiloride (Figure 2a). In contrast, the addition of lithium with or without amiloride to the basolateral compartment did not change AQP2 levels. Similar results were obtained with another ENaC blocker, benzamil (Figure 2b).

If ENaC is the main entry site for lithium, cellular uptake of lithium and the lithium-induced downregulation of AQP2 should be influenced by the sodium concentration. In pilot experiments, $mCCD_{c11}$ cells were grown in medium containing lower concentrations of sodium at the apical side for variable time periods. Incubation of the cells for 12 h in medium containing 60, 90, or 150 mM sodium showed similar AQP2 expression, whereas lower concentrations of sodium or more prolonged incubations resulted in the reduction of AQP2 expression (data not shown). Therefore, we incubated the cells with lithium for 12 h in the presence of 150, 90, or 60 mM sodium. Indeed, the AQP2 expression negatively correlated to the sodium concentration (Figure 2c), thus confirming competition between sodium and lithium, and indicating that lithium enters the cells through a sodium-transporting protein.

If ENaC is the apical entry site for lithium, amiloride should reduce transcellular transport and the intracellular concentration of lithium. To test this, cells were treated with 10 mM lithium at the apical side with or without amiloride. After 24 h, we observed a significant decrease in the lithium concentration at the apical side and an increase at the basolateral side, indicating that transcellular lithium transport occurred, which was inhibited by co-incubation with amiloride (Figure 3a). We next determined intracellular lithium levels. A 24-h incubation of cells with 1 mM lithium at the basolateral side resulted only in an intracellular lithium concentration of 3 ± 3 pmol lithium per μg protein, which corresponds to a $[Li^+]_i$ of 0.7 mM (Figure 3b). This is well above that of control cells (below detection limit; data not shown), indicating that some lithium enters the cells from the basolateral side. Intracellular lithium concentrations were markedly higher when 1 or 10 mM lithium was also added to the apical side, resulting in concentrations of 3.0 and 26.0 mM, respectively. In the presence of amiloride, intracellular lithium concentrations were reduced by more than 75%. To determine whether the obtained data were cell line-specific, we repeated some of the above experiments in $mpkCCD_{cl4}$ cells. In these cells, amiloride also reduced the intracellular lithium concentration and prevented lithium-induced downregulation of AQP2 (Supplementary Figure S1).

Together, these data indicate that ENaC is the main cellular entry site for lithium in collecting duct cells and that blocking ENaC by amiloride prevents lithium-induced downregulation of AQP2.

Effects of lithium and amiloride on ENaC subunit expression

In vivo, it has been shown that lithium treatment results in the ENaC downregulation.[21] To see whether similar effects occurred *in vitro*, $mCCD_{c11}$ cells were treated with lithium for

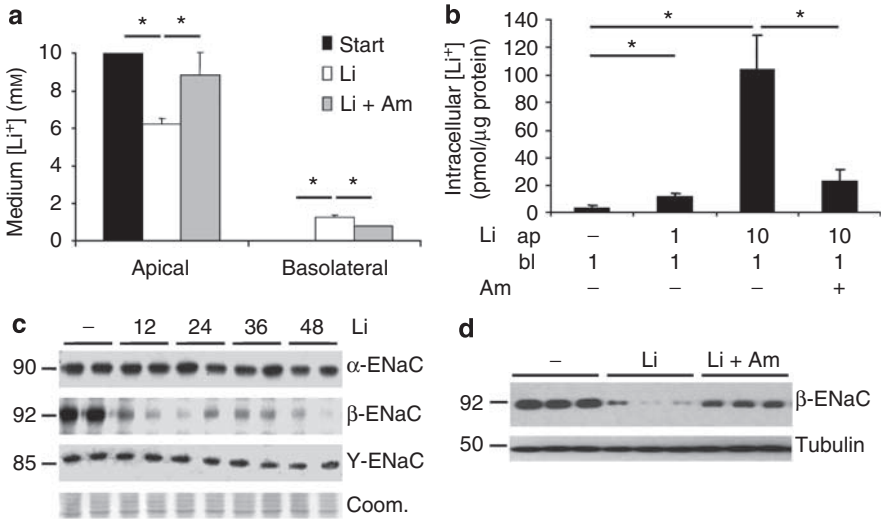

Figure 3 | Amiloride blocks lithium transport. mCCD$_{c11}$ cells were grown as previously described. (**a**) After a 24-h treatment with 10 mM lithium with/without amiloride at the apical side, media from the apical and basolateral compartments were collected and lithium concentrations were determined. (**b**) mCCD$_{c11}$ cells were treated for the last 24 h with the indicated concentrations of lithium at the basolateral (bl) and/or apical (ap) side in the absence or presence of 10 µM amiloride. After 24 h, lithium concentrations were determined. Intracellular lithium concentrations were corrected for contamination with extracellular lithium and normalized for the amount of protein. (**a**,**b**) The mean lithium concentration ([Li^+] ± s.e.m. in mM (**a**) or in pmol/µg protein (**b**)) was determined from at least three independent filters per condition. Significant difference *$P<0.05$. (**c**) mCCD$_{c11}$ cells were treated with lithium on the apical (10 mM) and basolateral (1 mM) side for the indicated time periods, lysed, and analyzed for ENaC subunit expression. (**d**) mCCD$_{c11}$ cells were treated as in panel c with or without amiloride for 24 h and analyzed for β-ENaC. (**c** and **d**) Molecular masses (in kDa) are indicated on the left. Significant differences ($P<0.05$) from control are indicated by an asterisk.

12–48 h. Indeed, lithium reduced the expression of β-ENaC, but not of α- or γ-ENaC (Figure 3c). However, these cells showed an amiloride-dependent transcellular voltage (data not shown), indicating that ENaC was still functionally expressed. Amiloride partially prevented the downregulation of β-ENaC (Figure 3d).

Effects of lithium and amiloride on GSK3β

Rao *et al.*[22] showed a decreased glycogen synthase kinase (GSK)3β activity in lithium-treated rats, suggesting a possible involvement of GSK3β in the pathway leading lithium-NDI. To test whether GSK3β is also involved in the lithium-induced downregulation of AQP2, total GSK3β expression and the extent of GSK3β-inactivating phosphorylation at Ser9 were analyzed in conjunction with AQP2 expression. Although lithium treatment for 48 h again caused downregulation of AQP2, it did not change total GSK3β expression levels, but strongly increased the Ser9 phosphorylation of GSK3β (Figure 4a). Zinc also inhibits GSK3β,[23] and BIO-Acetoxime is a specific GSK3 inhibitor.[24,25] Indeed, similar to lithium, 20 µM, but not 1 µM, zinc reduced AQP2 levels and increased phosphorylated GSK3β, but did not affect total GSK3β levels (Figure 4a). In line with an important role of GSK3β in AQP2 expression, BIO-Acetoxime also decreased the expression of AQP2 (Figure 4b).

As amiloride prevents lithium-induced downregulation of AQP2, we also tested whether amiloride reduced the effect of lithium on GSK3β. Indeed, although amiloride again protected the lithium-induced downregulation of AQP2, it did not affect total GSK3β expression, but significantly reduced the extent of lithium-induced phosphorylation of GSK3β at Ser9 (Figure 4c).

Together, these data strongly suggest that in mpkCCD$_{cl4}$ cells, lithium affects AQP2 expression by inactivating GSK3β through the phosphorylation at Ser9, which is attenuated by amiloride.

The effect of amiloride on the development of lithium-NDI in rats

To analyze whether amiloride can prevent the development of lithium-NDI *in vivo*, rats were fed on lithium chow for 4 weeks, with or without amiloride, whereas control rats fed on normal chow. All rats had free access to a salt block to compensate for the sodium losses that occur in lithium-NDI.[26]

As anticipated,[7,8] the rats treated with lithium developed severe polyuria with reduced urine osmolality (Table 1). Amiloride treatment attenuated this polyuria and increased urine osmolality compared with lithium only. Serum lithium concentrations found in the lithium (0.69 ± 0.08 mM) and lithium–amiloride (0.57 ± 0.08 mM) groups were similar and in the therapeutic range, whereas serum lithium concentrations in control rats were below the detection limit (0.05 mM; Table 1). As observed more often,[7,27–30] lithium-treated rats had a slightly lower body weight. We observed no differences in serum sodium or serum creatinine concentrations. However, there were differences in the urinary excretion of the various solutes. Lithium treatment resulted in increased sodium losses, which was further exaggerated by amiloride,

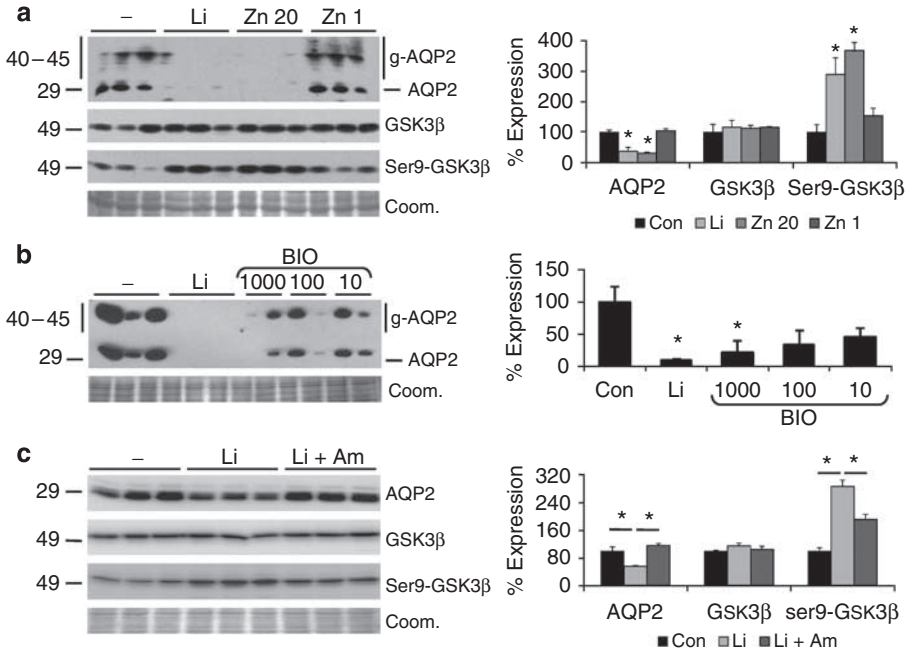

Figure 4 | Effects of lithium on GSK3β. Confluent mpkCCD$_{cl4}$ monolayers were treated for 96 h with 1 nM dDAVP. (**a**) Cells were treated with 1 mM lithium at the basolateral side and 10 mM lithium at the apical side, or with 20 and 1 μM zinc at both sides for the last 48 h and subjected to AQP2, GSK3β, and phospho-GSK3β(Ser9) immunoblotting or, after blotting, stained with coomassie blue. (**b**) mpkCCD$_{cl4}$ cells were treated with a specific GSK3-inhibitor (BIO-Acetoxime) for the last 48 h and subjected to AQP2 immunoblotting. Concentrations are expressed in nanomolar. (**c**) Cells were incubated for the last 48 h in the absence or presence of lithium with or without 10 μM amiloride as indicated. At the basolateral and apical side, 1 and 10 mM lithium were used, respectively. Molecular masses (in kDa) are indicated on the left. Semiquantification, normalization, and statistical analysis were carried out as described in the legend of Figure 1. Significant differences ($P < 0.05$) from control are indicated by an asterisk.

Table 1 | Blood and urine parameters

	–	Li	Li + Am
Body weight (g)	287 ± 11	212 ± 7*	232 ± 8*
Plasma osmolality (mOsm)	283 ± 5	304 ± 5*	288 ± 3**
Plasma lithium (mmol/l)	/	0.69 ± 0.08	0.57 ± 0.08
Plasma sodium (mmol/l)	141 ± 1	142 ± 2	141 ± 2
Plasma urea (mmol/l)	5.9 ± 0.3	4.0 ± 0.3*	5.6 ± 0.7
Plasma creatinine (μmol/l)	43 ± 3	41 ± 1	41 ± 2
Urine volume (ml/day)	13 ± 2	189 ± 15*	108 ± 24*,**
Urine osmolality (mOsm)	1537 ± 158	98 ± 25*	400 ± 93*,**
Total lithium excretion (mmol/24 h)	/	0.38 ± 0.10	0.61 ± 0.10
Total sodium excretion (mmol/24 h)	1.5 ± 0.3	4.7 ± 0.2*	11.4 ± 1.9*,**
Total potassium excretion (mmol/24 h)	3.2 ± 0.5	2.4 ± 0.4	3.0 ± 0.3
Total urea excretion (mmol/24 h)	10.9 ± 0.2	6.8 ± 0.5	8.6 ± 1.3
Osmolar excretion (mOsm/24 h)	18.3 ± 0.2	16.9 ± 0.3	35.4 ± 6.7
Creatinine clearance (ml/min)	0.93 ± 0.05	0.42 ± 0.09*	0.72 ± 0.12
Urea clearance (ml/min)	1.31 ± 0.25	1.20 ± 0.07	1.15 ± 0.17
Lithium clearance (ml/min)	/	0.65 ± 0.10	0.98 ± 0.25

Am, amiloride; Li, lithium.
Values are means ± s.e.m.
*Significant differences between control (–) and other groups.
**Significant differences between the lithium (Li) and lithium+amiloride group (Li+Am).
/ Below detection limit.

confirming the need for the salt block. To investigate whether there were differences in food intake, the excretion of potassium and urea was measured. Urinary excretion of these solutes was numerically, although not significantly, lower in rats treated with lithium only. In rats treated with lithium and amiloride, values were similar to controls. Furthermore, creatinine clearance was lower in lithium-treated rats than in control rats. This was not the case in the amiloride–lithium-treated rats.

The effect of amiloride on the renal collecting duct in lithium-NDI rats

Lithium-NDI is characterized by a decreased fraction of AQP2-expressing principal cells with a parallel increase of

H-ATPase-expressing intercalated cells.[7] We evaluated the effect of amiloride treatment on AQP2 and H-ATPase expression and on the cellular composition in different regions of the kidney. We observed a significantly reduced expression of AQP2 in the cortex of lithium-treated animals (Figure 5; Table 2). Amiloride significantly attenuated this decrease, but did not restore the AQP2 expression to the level of untreated rats. Similar results were obtained for the outer and inner medulla (Table 2). With respect to the expression of H-ATPase, we noted an increased expression in the cortex of lithium-treated rats, which was prevented by amiloride (Figure 5). Similar data were obtained for the outer and inner medulla (Table 2).

To investigate whether amiloride treatment also affects the ratio of principal and intercalated cells, kidney sections were labeled with antibodies against AQP2, H-ATPase, and nuclear TOTO-3. In agreement with earlier studies[7,8] and with the immunoblot data, lithium treatment resulted in a decreased density of AQP2-expressing cells and an increased density of H-ATPase-expressing cells (Figure 6a). Amiloride treatment attenuated these changes.

We quantified the changes by calculating a principal/intercalated cell ratio. Lithium treatment significantly reduced the ratio in the cortex, an effect that was fully prevented by amiloride (control: 1.72 ± 0.09; lithium: 0.83 ± 0.06; and lithium–amiloride: 1.78 ± 0.15; Figure 6b).

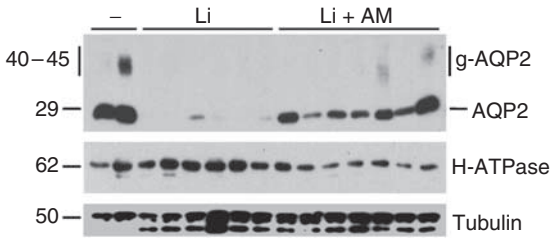

Figure 5 | Amiloride prevents effects of lithium on AQP2 and H-ATPase expressions in lithium-NDI rats. Wistar rats were fed a normal diet (–; $n = 6$), a diet containing lithium (Li; $n = 6$), or a diet containing lithium and amiloride (Li + Am; $n = 7$). After 4 weeks, one kidney was divided in the cortex, outer medulla, and inner medulla segments and solubilized. An equal amount of protein of the cortex of each rat was immunoblotted for AQP2, H-ATPase, or tubulin (indicated). Molecular masses (in kDa) are indicated on the left.

Table 2 | Effect of amiloride on collecting duct marker protein expression

	AQP2			H-ATPase		
	–	Li	Li + Am	–	Li	Li + Am
Cortex	100 ± 6	4 ± 2*	22 ± 4*,**	100 ± 42	303 ± 23*	150 ± 19**
Outer medulla	100 ± 5	30 ± 9*	53 ± 6*,**	100 ± 30	179 ± 17*	121 ± 40
Inner medulla	100 ± 4	6 ± 4*	42 ± 4*,**	100 ± 29	129 ± 13	65 ± 20**

Am, amiloride; Li, lithium.
Mean values (± s.e.m.) are expressed as percentages of the controls.
*Significant differences between control (–) and other groups.
**Significant differences between the lithium (Li) and lithium + amiloride group (Li + Am).

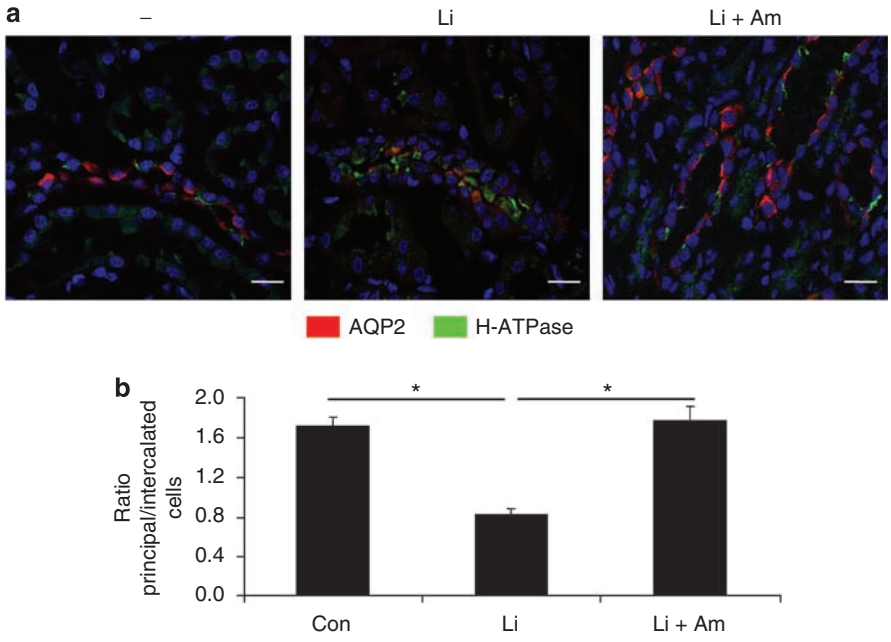

Figure 6 | Amiloride prevents cell conversion in lithium-NDI rats. (**a**) Of the rats described in the Figure 5 caption, one kidney was removed and fixed. Cryosections were prepared and incubated with rabbit H-ATPase (green) and guinea pig AQP2 (red) antibodies, followed by Alexa-488-conjugated goat-anti-rabbit and Alexa-594-conjugated goat anti-guinea pig antibodies. TOTO-3 (blue) was used to counterstain the sections. Images were produced with confocal laser scanning microscopy. Bars = 10 μm. (**b**) Of >5 defined areas of the kidney cortex of each control ($n = 6$), lithium ($n = 6$), and lithium + amiloride ($n = 7$) rats, cells positive for AQP2 or H-ATPase were counted and expressed as the ratio of principal and intercalated cells (± s.e.m.) (total cells control (–): 1244; Li: 1393; Li + Am: 2064). Significant differences *$P < 0.05$.

Similar results were obtained for the outer medulla (control: 2.21 ± 0.15; lithium: 1.02 ± 0.07; and lithium–amiloride: 1.98 ± 0.13) and the inner medulla (control: 2.66 ± 0.56; lithium: 1.16 ± 0.12; and lithium–amiloride: 1.91 ± 0.07), indicating that amiloride prevents the change in the ratio of principal/intercalated cells.

DISCUSSION

$mCCD_{c11}$ cells are a proper model to study lithium-induced AQP2 downregulation

A major impediment to the study of lithium-NDI at the cellular level was the lack of a suitable model. Our study indicates that $mCCD_{c11}$ cells are an appropriate model for the following reasons. First, $mCCD_{c11}$ cells express all three ENaC subunits in the apical membrane and show amiloride-inhibitable sodium transport.[20] Second, and similar to collecting duct cells *in vivo*, $mCCD_{c11}$ cells show a dDAVP-dependent increase in the expression of endogenous AQP2 (Figure 1a). Third, and in line with *in vivo* findings,[5] $mCCD_{c11}$ cells show a time- and concentration-dependent decrease in the AQP2 expression in response to therapeutically relevant lithium concentrations (Figure 1b).

ENaC is the main entry site for lithium and blocking ENaC prevents lithium-induced GSK3β inactivation and AQP2 downregulation *in vitro*

With 1 mM lithium added to the basolateral side of $mCCD_{c11}$ cells, a small but significant increase in the intracellular lithium concentration was observed (Figure 3b). As the cells formed a tight monolayer, this indicated that lithium can enter through a basolateral site. Although the identity of this entry pathway remains to be established, it did not reduce AQP2 expression (Figure 2a).

Upon addition of 1 mM lithium to the apical compartment, intracellular lithium concentrations increased about 3.5-fold to 3.0 mM (Figure 3b), which resulted in slightly, but not significantly, reduced AQP2 levels (Figure 1b). The addition of 10 mM lithium together with amiloride to the apical compartment resulted in similar intracellular lithium concentrations (Figure 3b) and in normal AQP2 levels (Figure 2a). In contrast, the AQP2 expression was strongly reduced with 10 mM lithium at the apical side in the absence of amiloride (Figure 1c), which coincided with an intracellular lithium concentration of 26 mM (Figure 3b). The observed AQP2 reduction suggests that within 24 h, AQP2 expression is downregulated with a threshold of intracellular lithium concentrations between 3 and 26 mM, which are obtained with lithium concentrations of 1 mM at the basolateral side and 10 mM at the apical side. However, at prolonged incubation times, AQP2 downregulation may be induced with lower extracellular lithium concentrations, as illustrated by the reduced AQP2 levels upon incubation with 1 mM lithium for 48 h (Figure 1b). In agreement with an important role of GSK3β activity in lithium-NDI mice[22] and the protective effect of amiloride on lithium-induced downregulation of AQP2, lithium, and also other GSK3β inhibitors, increased inactivating GSK3β phosphorylation and downregulation of AQP2 expression in $mpkCCD_{cl4}$ cells, which was partially prevented by co-treatment with amiloride (Figure 4).

The observed intracellular lithium concentration of 26 mM is higher than the concentration in the extracellular fluid, which has been observed before.[31] Immunocytochemistry did not show the difference in cell size between lithium-treated and control cells, and, in similar experiments, intracellular potassium levels were not different between control, lithium- and lithium + amiloride-treated cells, indicating that this is not because of an increased intracellular volume in the lithium-treated cells. More likely, the strong inwardly directed electrochemical potential for lithium and the fact that lithium is a poor substitute for sodium with Na/K-ATPase to be transported to the extracellular fluid[32] cause intracellular accumulation of lithium.

Overall, our study provides strong evidence that ENaC is the major cellular entry pathway for lithium and that blocking ENaC reduces lithium-induced GSK3β inactivation and prevents AQP2 downregulation.

Co-treatment with amiloride attenuates lithium-NDI

As reported,[5,7] lithium also induced NDI in our experiments, as indicated by the increased urine volume and decreased urine osmolality (Table 1). Our data furthermore reveal that amiloride treatment decreased urine volume and increased urine osmolality (Table 1). Although these changes point to a better urine-concentrating ability, the observed changes could theoretically be due to differences in solute intake or extracellular volume: an increased solute intake increases urine volume because of osmotic diuresis, whereas hypovolemia will reduce urine volume and increase urine osmolality. However, our data clearly indicate that the effects of amiloride cannot be explained by these factors. First, the urinary excretion of osmolytes was higher in the amiloride-lithium group than in the group receiving lithium only. Second, if anything, volume depletion was more likely to be present in lithium-only-treated rats as suggested by the lower body weight, and the reduction in creatinine clearance.

Consistent with this and the protective effect of amiloride in $mCCD_{c11}$ cells, rats treated with amiloride and lithium had significantly increased AQP2 and decreased H-ATPase expression compared with rats treated with lithium only (Figures 5 and 6; Table 2), and the lithium-induced change in the principal/intercalated cell ratio was completely prevented (Figure 6). Taken together, our data indicate that amiloride has a protective effect on lithium-NDI development by preventing the lithium-induced change in the cellular composition and partial protection of AQP2 downregulation, leading to a preserved concentrating ability of the collecting duct.

The complete prevention of the change in the cell ratio and the partial protection of AQP2 downregulation by amiloride suggests that AQP2 expression is more sensitive to lithium than the integrity of the principal cells, which is in

agreement with the fact that AQP2 downregulation precedes the fractional decrease in principal cells in lithium-NDI development.[4,8] It furthermore suggests that the used amiloride concentration did not completely prevent the deleterious effect of lithium, and it is unclear whether a residual effect of lithium can explain the fact that the concentrating ability of amiloride-treated rats is still lower than in control rats. One explanation for the reduced concentrating ability is that blockage of sodium reabsorption by amiloride could lead to a decrease in osmolality in the interstitium. However, considering the small contribution of sodium transport through ENaC to the interstitial osmolality, which is even less when NaCl is given *ad libitum* as done here, this is rather unlikely.

Alternatively, this could be due to an incomplete block of ENaC by amiloride in the kidney or due to cellular lithium influx through (an) other transporter(s)/channel(s). Amiloride was added to the food of the rats at a concentration of 200 mg/kg dry food, which is equivalent with 5 mg of amiloride. Assuming a volume of distribution of 3.4 l/kg and a $t½$ of 21 h, and a bioavailability of 10%,[33,34] this will lead to a plasma concentration of 3 μM. Amiloride clearance has been estimated to be about three times the creatinine clearance,[35] leading to a amiloride excretion of 9 μmol/day and an end-urine concentration of 84 μM, which, as the IC_{50} of amiloride is 0.1–0.5 μM,[36] very likely completely blocks ENaC. If these calculations hold for our rats, our data suggest that, in line with our *in vitro* data, some lithium may enter principal cells through a protein other than ENaC.

In our lithium-induced NDI rats and as observed by others,[8] we observed an increased expression of H-ATPase, which can be partly attributed to an increase in the number of intercalated cells (Figures 5 and 6). It has been suggested that the observed reduction in AQP2 expression with lithium is partially due to a loss of principal cells, either by differentiation of principal cells to intercalated cells or by selective cell death of principal cells.[7,8] Occasionally, and as observed by others,[7] we observed cells to stain positive for both AQP2 and H-ATPase, which may suggest that the change of the principal/intercalated cell ratio in lithium-NDI is (partly) due to a transition of principal to intercalated cells. However, the numbers were too low to influence the counting of the principal/intercalated cell ratio. In line with a loss of principal cells, Christensen *et al.*[8] found an increased number of apoptosis-inducing factor-labeled collecting duct cells in the inner medullary collecting duct after 10 and 15 days of lithium treatment, suggesting that apoptosis of principal cells may be involved, at least in part, in the changes in cellular composition in lithium-induced NDI. However, they also found an increased proliferation of not only intercalated cells but also principal cells, and, therefore, the change in cell composition could be the result of an increased number of intercalated cells without a loss of principal cells. If so, the reduced expression of AQP2 could be the result of a decreased expression per cell only. The exact underlying mechanism awaits further experiments.

Lithium-NDI also coincides with reduced expression of urea transporters UT-A1 and UT-B, and Bedford *et al.*[37,38] recently showed that amiloride treatment also significantly increases UT-A1 expression and conserves the osmotic gradient compared with rats treated with lithium only. Considering our data, the changes in UT-A1 expression and osmotic gradient with lithium and lithium–amiloride, respectively, could be due to a decreased/increased expression per cell, but are likely (partially) explained by the changes in the principal/intercalated cell ratio.

In conclusion, our data reveal that $mCCD_{cl1}$ cells form a proper model to study lithium-NDI. We show that ENaC forms the major entry pathway for lithium into principal cells, and that blocking ENaC with amiloride reduces the lithium-induced AQP2 downregulation, protects the cellular composition of the collecting duct, and thereby attenuates lithium-NDI. As such, our data provide a rationale for the use of amiloride in treating lithium-NDI patients.

MATERIALS AND METHODS

Cell culture

Mouse $mCCD_{cl1}$ and $mpkCCD_{cl4}$ cells were essentially grown as described.[20,39] Cells were seeded at a density of 1.5×10^5 cells/cm^2 on semi-permeable filters (Transwell, 0.4 μm pore size; Corning Costar, Cambridge, MA, USA) and cultured for 8 days. Unless stated otherwise, the cells were treated for the last 96 h with 1 nM dDAVP to the basolateral side, to induce AQP2 expression. Lithium and zinc chloride were administered as indicated. A concentration of 10 μM of amiloride or benzamil, concentrations specifically blocking ENaC,[36,40] were administered to the apical side, unless indicated otherwise. BIO-Acetoxime (Calbiochem, San Diego, CA, USA) was used indicated. Medium with reduced sodium concentrations was prepared identical to the standard medium except that lower amounts of NaCl were added.

Lithium assays

To determine transcellular lithium transport, $mCCD_{cl1}$ cells were grown on 1.13 cm^2 filters. After 24 h treatment with 10 mM lithium in the presence or absence of amiloride at the apical side, the basolateral and apical media were collected and the lithium concentrations were determined with a flame photometer (Eppendorf 6341, Hamburg, Germany).

Intracellular lithium concentrations were determined essentially as described.[31] Briefly, $mCCD_{cl1}$ cells were grown on 4.7-cm^2 filters. To determine the extent of lithium contamination from the extracellular side, fluorescein isothiocyanate dextran (FITC-dextran) was added to the lithium-containing medium to a final concentration of 10 μM just before harvesting, after which the medium was mixed. Then, the filters were washed three times with iso-osmotic sucrose (pH 7.3) at 4 °C and cells were lysed by sonication in 1 ml Milli-Q water. Of the 800 μl sample, the amount of lithium was determined by flame photometry, from which the total amount of lithium in the sample was calculated.

Of the 100 μl sample, the amount of FITC-dextran was measured using spectrofluorophotometry (Shimadzu RF-5301, Kyobo, Japan) at 492 nM (excitation) and 518 nm (emission) wavelengths. By comparing the obtained values with a two-fold FITC-dextran dilution series, the FITC-dextran concentration in each sample was determined, from which the extent of extracellular

Li^+ contamination was calculated and subtracted from the total amount to obtain the intracellular lithium amount. With the used FITC-dextran concentration, a contamination above 1:5000 would be detected. To correct for differences in cellular yield, the intracellular lithium amounts were normalized for the protein amount in each sample, which was determined using the Bio-Rad Protein Assay (Munchen, Germany). The intracellular lithium concentration (in millimolar) was estimated by calculating the cellular water content, on the basis of the assumption that 20% of the cell weight consists of cellular proteins and the remaining 80% is water.[41]

Experimental animals

Male Wistar rats (200–300 g) were obtained from the Animal Facility of the RUNMC (Radboud University Nijmegen Medical Centre). The rats were treated with lithium as described.[5]

Control rats received normal rodent diet (ssniff R/M-H V1534, ssniff Spezialdiaten GmbH, Soest, Germany; $n=6$). For lithium therapy, lithium chloride was added to the chow to give a concentration of 40 mmol/kg for the first week and 60 mmol/kg dry food for the next 3 weeks. The rats were then killed ($n=6$). For amiloride treatment, amiloride was added to the lithium chow to a concentration of 200 mg/kg dry food for the entire 4 weeks ($n=7$). All rats had free access to water, food, and a sodium-chloride block.[7] For the last 48 h of the experiment, the rats were housed in metabolic cages to measure water intake and urine output during the last 24 h. All animal experiments were approved by the Animal Experiments Committee of the RUNMC.

Tissue preparation

Rats were anesthetized with isofluorothane, after which their blood was removed by a heart puncture. Then, the rats were killed by cervical dislocation and the kidneys rapidly removed. One kidney was fixed for immunohistochemistry by immersion in 1% (wt/vol) periodate-lysine-paraformaldehyde for 2 h and in 15% (wt/vol) sucrose in phosphate buffered saline overnight, whereas of the other kidney, the inner medulla, outer medulla, and cortex were dissected for immunoblotting as described.[19]

Blood and urine analyses

Blood serum was prepared by 16 h incubation at 4 °C, followed by centrifugation at 600 *g* for 2–3 min. Urine was centrifuged at 4000 *g* for 5 min to remove sediment. Both serum and urine samples were analyzed for osmolality, and for sodium and lithium concentrations by standard procedures of the General Clinical Chemical laboratory of the RUNMC.

Immunoblotting

$mCCD_{cl1}$ cells from the 1.13 cm^2 filter were lysed in 200 µl Laemmli buffer and 15 µl samples were analyzed, while 5–10 µg of kidney material was also analyzed. Polyacrylamide gel electrophoresis, blotting, and blocking of the PVDF membranes were carried out as described.[42] The membranes were incubated for 16 h with affinity-purified rabbit AQP2 antibodies (1:3000 dilution),[43] affinity-purified rabbit anti-v1 H-ATPase antibodies (1:2000-dilution; gift from Dr S Nielsen, Denmark), rabbit anti-Ser9-GSK3β (1:1000 dilution; Cell Signaling Technology, Beverly, MA, USA), mouse anti-GSK3β (1:5000 dilution; BD Transduction Laboratories, San Jose, CA, USA), or with mouse anti-tubulin antibodies (1:100,000 dilution; gift from Dr Kreis, Switzerland) in Tris-buffered saline Tween-20 supplemented with 1% non-fat dried milk. ENaC detection was carried out as described.[20] Blots were incubated for 1 h with goat anti-rabbit IgGs (1:5000) or with goat anti-mouse IgGs (1:2000) (Sigma, St Louis, MO, USA) as secondary antibodies coupled to horseradish peroxidase. Proteins were visualized using enhanced chemiluminescence (Pierce, Rockford, IL, USA). Films were scanned using a Bio-Rad 690c densitometer and signals were analyzed using Bio-Rad software. Two-fold dilution series of the respective proteins were blotted in parallel to allow semi-quantification. Equal loading of the samples was confirmed by parallel immunoblotting for tubulin or by staining of the blots with coomassie blue.

Immunohistochemistry

Immunohistochemical staining was performed on 7-µm-thick sections of fixed frozen kidney samples, following antigen retrieval. The sections were blocked in goat serum dilution buffer (GSDB: 16% goat serum, 0.3% Triton X-100, 0.3 M NaCl in phosphate buffered saline) for 30 min and incubated for 16 h at 4 °C with rabbit anti-a4 H-ATPase antibodies (1:3000, provided by Dr F Karet, UK). After washes and incubation with Alexa 488-conjugated goat anti-rabbit antibodies, the sections were incubated with affinity-purified guinea pig AQP2 antibodies (1:50)[44] for 1 h at room temperature and with Alexa 594-conjugated goat anti-guinea pig secondary antibodies (Molecular Probes, Leiden, The Netherlands). TOTO-3 iodide (Invitrogen, Carlsbad, CA, USA) was used for counter-staining. Images were produced using Bio-Rad MRC-1024 confocal laser scanning microscopy.

Quantification of principal and intercalated cells was performed on the confocal images of the fluorescent kidney sections. Tubules in >5 randomly selected areas of each kidney region of each animal were included. Only cells with distinct TOTO-3 staining were counted. Cells stained with H-ATPase or AQP2 were considered as intercalated or principal cells, respectively.

Data analysis

Differences between groups were tested by Student's *t*-test corrected by the Bonferroni multiple-comparisons procedure. Differences were considered statistically significant for $P<0.05$.

DISCLOSURE

All the authors declared no competing interests.

ACKNOWLEDGMENTS

We thank Dr David Marples (Leeds, UK) and Dr Mark Knepper (NIH, Bethesda, MD, USA) for help with the setup of the animal studies. We thank Dr Fiona Karet (Cambridge, UK) for providing a4 H-ATPase antibodies and Dr Soren Nielsen (Aarhus, Denmark) for v1 H-ATPase antibodies. PMTD is a recipient of a VICI grant (865.07.002) from the Netherlands Organization for Scientific Research (NWO). This work was supported by RUNMC grants to PMTD (2004.55) and to PMTD and JFW (2005.48).

SUPPLEMENTARY MATERIAL

Figure S1. Effect of amiloride in $mpkCCD_{cl4}$ cells.
Supplementary material is linked to the online version of the paper at http://www.nature.com/ki

REFERENCES

1. Timmer RT, Sands JM. Lithium intoxication. *J Am Soc Nephrol* 1999; **10**: 666–674.
2. Boton R, Gaviria M, Batlle DC. Prevalence, pathogenesis, and treatment of renal dysfunction associated with chronic lithium therapy. *Am J Kidney Dis* 1987; **10**: 329–345.

3. Terris J, Ecelbarger CA, Nielsen S *et al.* Long-term regulation of four renal aquaporins in rats. *Am J Physiol* 1996; **40**: F414–F422.
4. Laursen UH, Pihakaski-Maunsbach K, Kwon TH *et al.* Changes of rat kidney AQP2 and Na,K-ATPase mRNA expression in lithium-induced nephrogenic diabetes insipidus. *Nephron Exp Nephrol* 2004; **97**: e1–16.
5. Marples D, Christensen S, Christensen EI *et al.* Lithium-induced downregulation of aquaporin-2 water channel expression in rat kidney medulla. *J Clin Invest* 1995; **95**: 1838–1845.
6. Mu J, Johansson M, Hansson GC *et al.* Lithium evokes a more pronounced natriuresis when administered orally than when given intravenously to salt-depleted rats. *Pflugers Arch* 1999; **438**: 159–164.
7. Christensen BM, Marples D, Kim YH *et al.* Changes in cellular composition of kidney collecting duct cells in rats with lithium-induced NDI. *Am J Physiol Cell Physiol* 2004; **286**: C952–C964.
8. Christensen BM, Kim YH, Kwon TH *et al.* Lithium treatment induces a marked proliferation of primarily principal cells in rat kidney inner medullary collecting duct. *Am J Physiol Renal Physiol* 2006; **291**: F39–F48.
9. Robben JH, Knoers NV, Deen PM. Cell biological aspects of the vasopressin type-2 receptor and aquaporin 2 water channel in nephrogenic diabetes insipidus. *Am J Physiol Renal Physiol* 2006; **291**: F257–F270.
10. Loffing J, Kaissling B. Sodium and calcium transport pathways along the mammalian distal nephron: from rabbit to human. *Am J Physiol Renal Physiol* 2003; **284**: F628–F643.
11. Kellenberger S, Gautschi I, Schild L. A single point mutation in the pore region of the epithelial Na+ channel changes ion selectivity by modifying molecular sieving. *Proc Natl Acad Sci USA* 1999; **96**: 4170–4175.
12. Singer I, Rotenberg D, Puschett JB. Lithium-induced nephrogenic diabetes insipidus: *in vivo* and *in vitro* studies. *J Clin Invest* 1972; **51**: 1081–1091.
13. Herrera FC, Beauwens R, Crabbe J. Mechanism of inhibition by lithium of sodium transport in the toad bladder. *Biol Cell* 1985; **55**: 257–263.
14. Thomsen K, Bak M, Shirley DG. Chronic lithium treatment inhibits amiloride-sensitive sodium transport in the rat distal nephron. *J Pharmacol Exp Ther* 1999; **289**: 443–447.
15. Wetzels JF, van Bergeijk JD, Hoitsma AJ *et al.* Triamterene increases lithium excretion in healthy subjects: evidence for lithium transport in the cortical collecting tubule. *Nephrol Dial Transplant* 1989; **4**: 939–942.
16. Batlle DC, von Riotte AB, Gaviria M *et al.* Amelioration of polyuria by amiloride in patients receiving long-term lithium therapy. *N Engl J Med* 1985; **312**: 408–414.
17. Kosten TR, Forrest JN. Treatment of severe lithium-induced polyuria with amiloride. *Am J Psychiatry* 1986; **143**: 1563–1568.
18. Bedford JJ, Weggery S, Ellis G *et al.* Lithium-induced nephrogenic diabetes insipidus: renal effects of amiloride. *Clin J Am Soc Nephrol* 2008; **3**(5): 1324–1331.
19. Li Y, Shaw S, Kamsteeg EJ *et al.* Development of lithium-induced nephrogenic diabetes insipidus is dissociated from adenylyl cyclase activity. *J Am Soc Nephrol* 2006; **17**: 1063–1072.
20. Gaeggeler HP, Gonzalez-Rodriguez E, Jaeger NF *et al.* Mineralocorticoid versus glucocorticoid receptor occupancy mediating aldosterone-stimulated sodium transport in a novel renal cell line. *J Am Soc Nephrol* 2005; **16**: 878–891.
21. Nielsen J, Kwon TH, Praetorius J *et al.* Segment-specific ENaC downregulation in kidney of rats with lithium-induced NDI. *Am J Physiol Renal Physiol* 2003; **285**: F1198–F1209.
22. Rao R, Zhang MZ, Zhao M *et al.* Lithium treatment inhibits renal GSK-3 activity and promotes cyclooxygenase 2-dependent polyuria. *Am J Physiol Renal Physiol* 2005; **288**: F642–F649.
23. Ilouz R, Kaidanovich O, Gurwitz D *et al.* Inhibition of glycogen synthase kinase-3beta by bivalent zinc ions: insight into the insulin-mimetic action of zinc. *Biochem Biophys Res Commun* 2002; **295**: 102–106.
24. Polychronopoulos P, Magiatis P, Skaltsounis AL *et al.* Structural basis for the synthesis of indirubins as potent and selective inhibitors of glycogen synthase kinase-3 and cyclin-dependent kinases. *J Med Chem* 2004; **47**: 935–946.
25. Meijer L, Skaltsounis AL, Magiatis P *et al.* GSK-3-selective inhibitors derived from Tyrian purple indirubins. *Chem Biol* 2003; **10**: 1255–1266.
26. Thomsen K. The effect of sodium chloride on kidney function in rats with lithium intoxication. *Acta Pharmacol Toxicol (Copenh)* 1973; **33**: 92–102.
27. Kwon TH, Laursen UH, Marples D *et al.* Altered expression of renal AQPs and Na(+) transporters in rats with lithium-induced NDI. *Am J Physiol Renal Physiol* 2000; **279**: F552–F564.
28. Rojek A, Nielsen J, Brooks HL *et al.* Altered expression of selected genes in kidney of rats with lithium-induced NDI. *Am J Physiol Renal Physiol* 2005; **288**: F1276–F1289.
29. Christensen S, Kusano E, Yusufi AN *et al.* Pathogenesis of nephrogenic diabetes insipidus due to chronic administration of lithium in rats. *J Clin Invest* 1985; **75**: 1869–1879.
30. Kotnik P, Nielsen J, Kwon TH *et al.* Altered expression of COX-1, COX-2, and mPGES in rats with nephrogenic and central diabetes insipidus. *Am J Physiol Renal Physiol* 2005; **288**: F1053–F1068.
31. Goldberg H, Clayman P, Skorecki K. Mechanism of Li inhibition of vasopressin-sensitive adenylate cyclase in cultured renal epithelial cells. *Am J Physiol* 1988; **255**: F995–1002.
32. Thomsen K, Shirley DG. A hypothesis linking sodium and lithium reabsorption in the distal nephron. *Nephrol Dial Transplant* 2006; **21**: 869–880.
33. Segre G, Cerretani D, Bruni G *et al.* Amiloride pharmacokinetics in rat. *Eur J Drug Metab Pharmacokinet* 1998; **23**: 218–222.
34. Baer JE, Jones CB, Spitzer SA *et al.* The potassium-sparing and natriuretic activity of *N*-amidino-3,5-diamino-6-chloropyrazinecarboxamide hydrochloride dihydrate (amiloride hydrochloride). *J Pharmacol Exp Ther* 1967; **157**: 472–485.
35. Spahn H, Reuter K, Mutschler E *et al.* Pharmacokinetics of amiloride in renal and hepatic disease. *Eur J Clin Pharmacol* 1987; **33**: 493–498.
36. Kleyman TR, Cragoe Jr EJ. Amiloride and its analogs as tools in the study of ion transport. *J Membr Biol* 1988; **105**: 1–21.
37. Klein JD, Gunn RB, Roberts BR *et al.* Down-regulation of urea transporters in the renal inner medulla of lithium-fed rats. *Kidney Int* 2002; **61**: 995–1002.
38. Bedford JJ, Leader JP, Jing R *et al.* Amiloride restores renal medullary osmolytes in lithium-induced nephrogenic diabetes insipidus. *Am J Physiol Renal Physiol* 2008; **294**: F812–F820.
39. Hasler U, Mordasini D, Bens M *et al.* Long-term regulation of aquaporin-2 expression in vasopressin-responsive renal collecting duct principal cells. *J Biol Chem* 2002; **277**: 10379–10386.
40. Simchowitz L, Cragoe Jr EJ. Inhibition of chemotactic factor-activated Na+/H+ exchange in human neutrophils by analogues of amiloride: structure–activity relationships in the amiloride series. *Mol Pharmacol* 1986; **30**: 112–120.
41. Erlinger SU, Saier Jr MH. Decrease in protein content and cell volume of cultured dog kidney epithelial cells during growth. *In Vitro* 1982; **18**: 196–202.
42. Kamsteeg EJ, Wormhoudt TA, Rijss JPL *et al.* An impaired routing of wild-type aquaporin-2 after tetramerization with an aquaporin-2 mutant explains dominant nephrogenic diabetes insipidus. *EMBO J* 1999; **18**: 2394–2400.
43. Deen PMT, Verdijk MAJ, Knoers NVAM *et al.* Requirement of human renal water channel aquaporin-2 for vasopressin-dependent concentration of urine. *Science* 1994; **264**: 92–95.
44. Deen PMT, van Aubel RA, van Lieburg AF *et al.* Urinary content of aquaporin 1 and 2 in nephrogenic diabetes insipidus. *J Am Soc Nephrol* 1996; **7**: 836–841.